1

What is the Mesoscale?

1.1 Space and time scales

Atmospheric motions occur over a broad continuum of space and time scales. The mean free path of molecules (approximately 0.1 μm) and circumference of the earth (approximately 40 000 km) place lower and upper bounds on the space scales of motions. The timescales of atmospheric motions range from under a second, in the case of small-scale turbulent motions, to as long as weeks in the case of planetary-scale Rossby waves. Meteorological phenomena having short temporal scales tend to have small spatial scales, and vice versa; the ratio of horizontal space to time scales is of roughly the same order of magnitude for most phenomena ($\sim$10 m s^{-1}) (Figure 1.1).

Before defining the mesoscale it may be easiest first to define the synoptic scale. Outside of the field of meteorology, the adjective *synoptic* (derived from the Greek *synoptikos*) refers to a "summary or general view of a whole." The adjective has a more restrictive meaning to meteorologists, however, in that it refers to large space scales. The first routinely available weather maps, produced in the late 19th century, were derived from observations made in European cities having a relatively coarse characteristic spacing. These early meteorological analyses, referred to as *synoptic maps*, paved the way for the Norwegian cyclone model, which was developed during and shortly after World War I. Because only extratropical cyclones and fronts could be resolved on the early synoptic maps, *synoptic* ultimately became a term that referred to large-scale atmospheric disturbances.

The debut of weather radars in the 1940s enabled phenomena to be observed that were much smaller in scale than the scales of motion represented on synoptic weather maps. The term *mesoscale* appears to have been introduced by Ligda (1951) in an article reviewing the use of weather radar, in order to describe phenomena smaller than the synoptic scale but larger than the *microscale*, a term that was widely used at the time (and still is) in reference to phenomena having a scale of a few kilometers or less.[1] The upper limit of the mesoscale can therefore be regarded as being roughly the limit of resolvability of a disturbance by an observing network approximately as dense as that present when the first synoptic charts became available, that is, of the order of 1000 km.

At least a dozen different length scale limits for the mesoscale have been broached since Ligda's article. The most popular bounds are those proposed by Orlanski (1975) and Fujita (1981).[2] Orlanski defined the mesoscale as ranging from 2 to 2000 km, with subclassifications of meso-α, meso-β, and meso-γ scales referring to horizontal scales of 200–2000 km, 20–200 km, and 2–20 km, respectively (Figure 1.1). Orlanski defined phenomena having scales smaller than 2 km as microscale phenomena, and those having scales larger than 2000 km as macroscale phenomena. Fujita (1981) proposed a much narrower range of length scales in his definition of mesoscale, where the mesoscale ranged from 4 to 400 km, with subclassifications of meso-α and meso-β scales referring to horizontal scales of 40–400 km and 4–40 km, respectively (Figure 1.1).

[1] According to Ligda (1951), the first radar-detected precipitation area was a thunderstorm observed using a 10-cm radar in England on 20 February 1941. Organized atmospheric science research using radars was delayed until after World War II, however, given the importance of the relatively new technology to military interests and the secrecy surrounding radar development.

[2] In addition to Orlanski and Fujita, scale classifications and/or subclassifications also have been introduced by Petterssen (1956), Byers (1959), Tepper (1959), Ogura (1963), and Agee *et al.* (1976), among others.

Mesoscale Meteorology in Midlatitudes Paul Markowski and Yvette Richardson

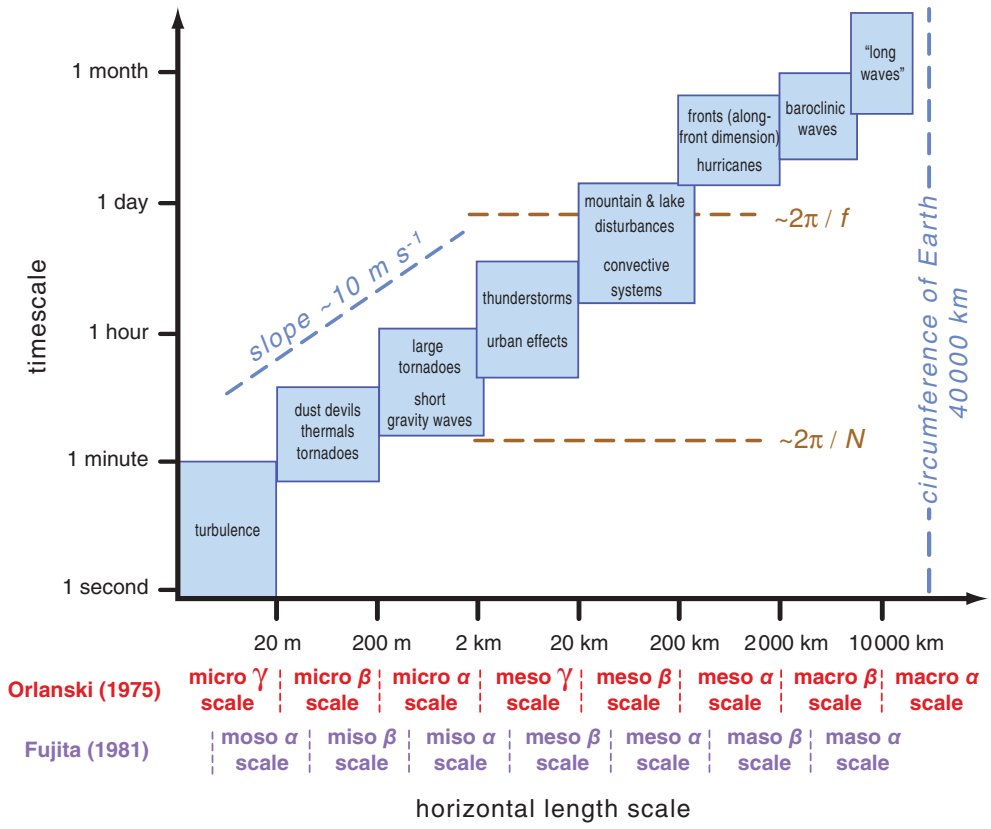

Figure 1.1 Scale definitions and the characteristic time and horizontal length scales of a variety of atmospheric phenomena. Orlanski's (1975) and Fujita's (1981) classification schemes are also indicated.

Fujita's overall scheme proposed classifications spanning two orders of magnitude each; in addition to the mesoscale, Fujita proposed a 4 mm–40 cm musoscale, a 40 cm–40 m mososcale, a 40 m–4 km misoscale, and a 400–40 000 km masoscale (the vowels A, E, I, O, and U appear in alphabetical order in each scale name, ranging from large scales to small scales). As was the case for Fujita's mesoscale, each of the other scales in his classification scheme was subdivided into α and β scales spanning one order of magnitude.

The specification of the upper and lower limits of the mesoscale does have some dynamical basis, although perhaps only coincidentally. The mesoscale can be viewed as an intermediate range of scales on which few, if any, simplifications to the governing equations can be made, at least not simplifications that can be applied to *all* mesoscale phenomena.[3] For example, on the synoptic scale, several terms in the governing equations can safely be disregarded owing to their relative unimportance on that scale, such as vertical accelerations and advection by the ageostrophic wind. Likewise, on the microscale, different terms in the governing equations can often be neglected, such as the Coriolis force and even the horizontal pressure gradient force on occasion. On the mesoscale, however, the full complexity of the unsimplified governing equations comes into play. For example, a long-lived mesoscale convective system typically contains large pressure gradients and horizontal and vertical accelerations of air, and regions of substantial latent heating and cooling and associated positive and negative buoyancy, with the latent heating and cooling profiles being sensitive to microphysical processes. Yet even the Coriolis force and radiative transfer effects have been shown to influence the structure and evolution of these systems.

The mesoscale also can be viewed as the scale on which motions are driven by a variety of mechanisms rather than by a single dominant instability, as is the case on

[3] This is essentially the same point as made by Doswell (1987).

the synoptic scale in midlatitudes.[4] Mesoscale phenomena can be either entirely topographically forced or driven by any one of or a combination of the wide variety of instabilities that operate on the mesoscale, such as thermal instability, symmetric instability, barotropic instability, and Kelvin-Helmholtz instability, to name a few. The dominant instability on a given day depends on the local state of the atmosphere on that day (which may be heavily influenced by synoptic-scale motions). In contrast, midlatitude synoptic-scale motions are arguably solely driven by baroclinic instability; extratropical cyclones are the dominant weather system of midlatitudes on the synoptic scale. Baroclinic instability is most likely to be realized by disturbances having a horizontal wavelength roughly three times the Rossby radius of deformation, L_R, given by $L_R = NH/f$, where N, H, and f are the Brunt-Väisälä frequency, scale height of the atmosphere, and Coriolis parameter, respectively.[5] Typically, L_R is in the range of 1000–1500 km. In effect, the scale of the extratropical cyclone can be seen as defining what synoptic scale means in midlatitudes.

In contrast to the timescales on which extratropical cyclones develop, mesoscale phenomena tend to be shorter lived and also are associated with shorter Lagrangian timescales (the amount of time required for an air parcel to pass through the phenomenon). The Lagrangian timescales of mesoscale phenomena range from the period of a pure buoyancy oscillation, equal to $2\pi/N$ or roughly 10 minutes on average, to a pendulum day, equal to $2\pi/f$ or roughly 17 hours in midlatitudes. The former timescale could be associated with simple gravity wave motions, whereas the latter timescale characterizes inertial oscillations, such as the oscillation of the low-level ageostrophic wind component that gives rise to the low-level wind maximum frequently observed near the top of nocturnal boundary layers.

The aforementioned continuum of scales of atmospheric motions and associated pressure, temperature, and moisture variations is evident in analyses of meteorological variables. Figure 1.2 presents one of Fujita's manual analyses (i.e., a hand-drawn, subjective analysis) of sea level pressure and temperature during an episode of severe thunderstorms.[6] Pressure and temperature anomalies are evident on a range of scales: for example, a synoptic-scale low-pressure center is analyzed, as are smaller-scale highs and lows associated with the convective storms. The magnitude of the horizontal pressure and temperature gradients, implied by the spacing of the isobars and isotherms, respectively, varies by an order of magnitude or more within the domain shown.

The various scales of motion or scales of atmospheric variability can be made more readily apparent by way of filters that preferentially damp select wavelengths while retaining others. For example, a *low-pass* filter can be used to remove relatively small scales from an analysis (*low-pass* refers to the fact that low-frequency [large-wavelength] features are retained in the analysis). A *band-pass* filter can be used to suppress scales that fall outside of an intermediate range. Thus, a low-pass filter can be used to expose synoptic-scale motions or variability and a band-pass filter can be used to expose mesoscale motions. (A *high-pass* filter would be used to suppress all but the shortest wavelengths present in a dataset; such filters are rarely used because the smallest scales are the ones that are most poorly resolved and contain a large noise component.) The results of such filtering operations are shown in Figure 1.3, which serves as an example of how a meteorological field can be viewed as having components spanning a range of scales. The total temperature field comprises a synoptic-scale temperature field having a southward-directed temperature gradient plus mesoscale temperature perturbations associated with thunderstorm outflow.

1.2 Dynamical distinctions between the mesoscale and synoptic scale

1.2.1 Gradient wind balance

On the synoptic scale, phenomena tend to be characterized by a near balance of the Coriolis and pressure gradient forces (i.e., geostrophic balance) for straight flow, so accelerations of air parcels and ageostrophic motions tend to be very small. For curved flow, the imbalance between these forces on the synoptic scale results in a centripetal acceleration such that the flow remains nearly parallel to the curved

[4] See, for example, Emanuel (1986).

[5] In addition to being related to the wavelength that maximizes the growth rate of baroclinic instability, L_R also is important in the problem of geostrophic adjustment. Geostrophic adjustment is achieved by relatively fast-moving gravity waves. The horizontal scale of the influence of the gravity waves is dictated by L_R, which physically can be thought of as the distance a gravity wave can propagate under the influence of the Coriolis force before the velocity vector is rotated so that it is normal to the pressure gradient, at which point the Coriolis and pressure gradient forces balance each other. For phenomena having a horizontal scale approximately equal to L_R, both the velocity and pressure fields adjust in significant ways to maintain/establish a state of balance between the momentum and mass fields. On scales much less than (greater than) L_R, the pressure (velocity) field adjusts to the velocity (pressure) field during the geostrophic adjustment process.

[6] Fujita called these mesoscale meteorological analyses *mesoanalyses*. The analyses he published over the span of roughly five decades are widely regarded as masterpieces.

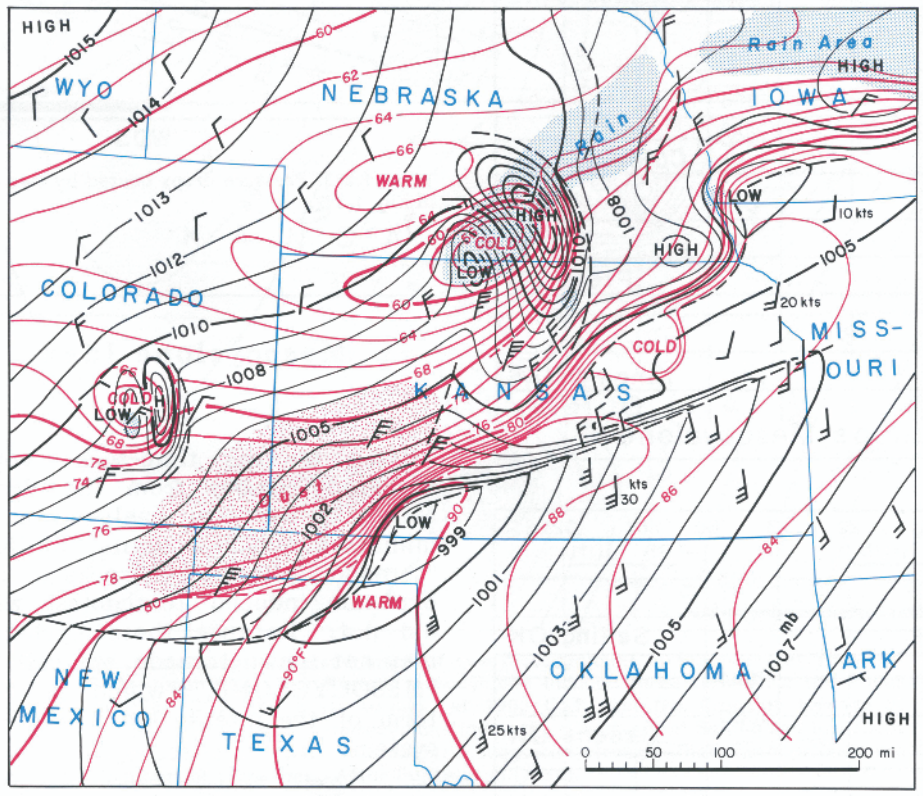

Figure 1.2 Sea-level pressure (black contours) and temperature (red contours) analysis at 0200 CST 25 June 1953. A squall line was in progress in northern Kansas, eastern Nebraska, and Iowa. (From Fujita [1992].)

isobars (i.e., gradient wind balance). Gradient wind balance is often a poor approximation to the air flow on the mesoscale. On the mesoscale, pressure gradients can be considerably larger than on the synoptic scale, whereas the Coriolis acceleration (proportional to wind velocity) is of similar magnitude to that of the synoptic scale. Thus, mesoscale systems are often characterized by large wind accelerations and large ageostrophic motions.

As scales decrease below ~1000 km the Coriolis acceleration becomes decreasingly important compared with the pressure gradient force, and as scales increase beyond ~1000 km ageostrophic motions become decreasingly significant. Let us consider a scale analysis of the horizontal momentum equation (the x equation, without loss of generality):

$$\frac{\mathrm{d}u}{\mathrm{d}t} = -\frac{1}{\rho}\frac{\partial p}{\partial x} + fv + F_u, \tag{1.1}$$

where u, v, ρ, p, f, $\mathrm{d}/\mathrm{d}t$, and F_u are the zonal wind speed, meridional wind speed, air density, pressure, Coriolis parameter, Lagrangian time derivative, and viscous effects acting on u, respectively. We shall neglect F_u for now, but we shall find later that effects associated with the F_u term are often important.

On the synoptic scale and mesoscale, for $O(v) \sim 10\ \mathrm{m\ s^{-1}}$, the Coriolis acceleration fv is of order

$$O(fv) \sim (10^{-4}\ \mathrm{s^{-1}})\,(10\ \mathrm{m\ s^{-1}}) \sim 10^{-3}\ \mathrm{m\ s^{-2}}.$$

On the synoptic scale, the pressure gradient force has a scale of

$$O\left(-\frac{1}{\rho}\frac{\partial p}{\partial x}\right) \sim \frac{1}{1\ \mathrm{kg\ m^{-3}}}\,\frac{10\ \mathrm{mb}}{1000\ \mathrm{km}} \sim 10^{-3}\ \mathrm{m\ s^{-2}};$$

thus, the Coriolis and pressure gradient forces are of similar scales and, in the absence of significant flow curvature, we can infer that accelerations ($\mathrm{d}u/\mathrm{d}t$) are small. Furthermore, because $v = v_g + v_a$ and $v_g = \frac{1}{\rho f}\frac{\partial p}{\partial x}$, where v_g and v_a are the geostrophic and ageostrophic meridional winds, respectively, (1.1) can be written as (ignoring F_u)

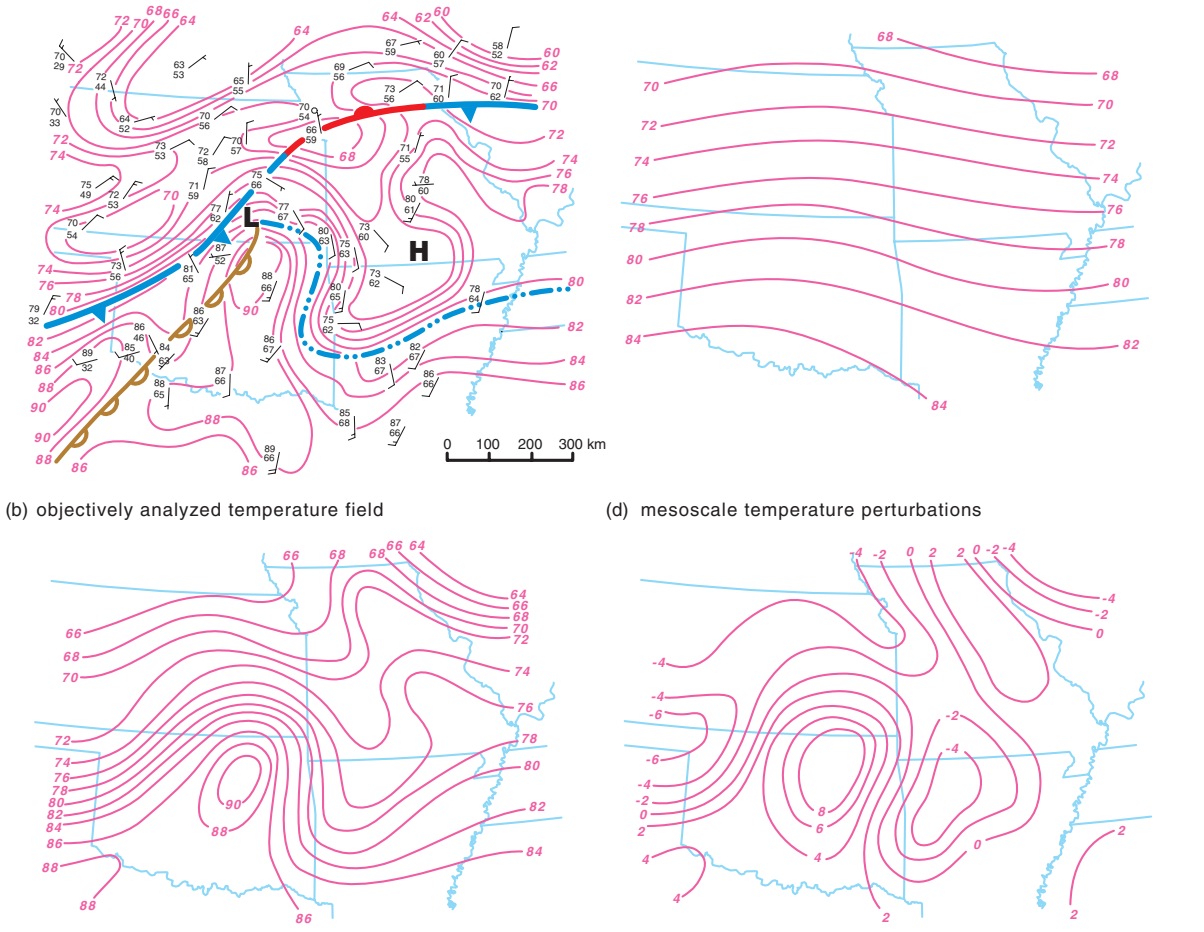

Figure 1.3 (a) Manual surface analysis for 2100 UTC 24 April 1975. Isotherms are drawn at 2 °F intervals and fronts and pressure centers are also shown. A thunderstorm outflow boundary is indicated using a blue dashed line with double dots. The brown boundary with open scallops denotes a dryline. (The symbology used to indicate outflow boundaries and drylines has varied from analyst to analyst; different symbols for outflow boundaries and drylines appear in other locations within this book.) (b) Computer-generated ('objective') analysis of the total temperature field, i.e., the sum of the synoptic-scale temperature field and the mesoscale temperature perturbations. The objectively analyzed total temperature field is fairly similar to the manually produced temperature analysis in (a), although some small differences can be seen. (c) The synoptic-scale temperature field (°F). This was obtained using a low-pass filter that significantly damped wavelengths smaller than approximately 1500 km. (d) Mesoscale temperature perturbation field (°F). This was obtained using a band-pass filter that had its maximum response for wavelengths of 500 km, and damped wavelengths much longer and much shorter than 500 km. (Adapted from Maddox [1980].)

$fv_a = -\frac{1}{\rho}\frac{\partial p}{\partial x} + fv$. Therefore, ageostrophic motions are also small on the synoptic scale (particularly for fairly straight flow), owing to the approximate balance between the Coriolis and pressure gradient forces, referred to as *quasigeostrophic balance*.

On the mesoscale, the horizontal pressure gradient, $\partial p/\partial x$, can range from 5 mb/500 km (e.g., in quiescent conditions) to 5 mb/5 km (e.g., beneath a thunderstorm). At the small end of this range, the Coriolis and pressure gradient forces may be approximately in balance, but at the large end of this range, the pressure gradient force is two orders of magnitude larger than on the synoptic scale (i.e., 10^{-1} m s^{-2} versus 10^{-3} m s^{-2}). On these occasions, the pressure gradient force dominates, the Coriolis force is relatively unimportant, and accelerations and ageostrophic motions are large.

A dimensionless number, called the *Rossby number*, assesses the relative importance of the Coriolis force and air parcel accelerations (the magnitude of the acceleration is directly related to the magnitude of the ageostrophic wind). The Rossby number can be used to distinguish synoptic-scale weather systems from subsynoptic-scale phenomena and is defined as

$$\mathrm{Ro} = \frac{O(\mathrm{d}\mathbf{v}/\mathrm{d}t)}{O(-f\mathbf{k}\times\mathbf{v})} \sim \frac{V/T}{fV} \sim \frac{V^2/L}{fV} \sim \frac{V}{fL}, \qquad (1.2)$$

where $\mathbf{k}$ is the unit vector in the positive z direction, T is a timescale (generally the advective timescale), V is the magnitude of a characteristic wind velocity, $\mathbf{v}$, and L is a characteristic horizontal length scale. On the synoptic scale, where the quasigeostrophic approximation usually can be made, Ro $\ll 1$. For mesoscale systems, Ro $\gtrsim 1$.

1.2.2 Hydrostatic balance

In many atmospheric applications (e.g., synoptic meteorology, large-scale dynamics) we assume that the atmosphere is in hydrostatic balance, that is, the vertical pressure gradient force per unit mass and gravitational acceleration are nearly balanced, resulting in negligible vertical accelerations. The vertical momentum equation can be written as

$$\frac{\mathrm{d}w}{\mathrm{d}t} = -\frac{1}{\rho}\frac{\partial p}{\partial z} + 2\Omega u\cos\phi - g + F_w, \qquad (1.3)$$

where w, g, Ω, ϕ, and F_w are the vertical velocity, gravitational acceleration, angular rotation rate of the earth, latitude, and viscous effects acting on w, respectively. The scale of g is 10 m s^{-2} and the scale of $|-\frac{1}{\rho}\frac{\partial p}{\partial z}|$ is also $\sim$(1 kg m^{-3})$^{-1}\cdot$ 100 mb/1000 m $\sim$ (1 kg m^{-3})$^{-1}\cdot 10^4$ Pa/10^3 m $\sim$ 10 m s^{-2}. We neglect F_w in this simple analysis, although F_w can be important, particularly near the edges of clouds and in rising thermals. Moreover, the contribution of the vertical component of the Coriolis force, $2\Omega u\cos\phi$, to vertical accelerations is often neglected as well (although its scale is not always negligible relative to the soon-to-be-defined buoyancy and vertical perturbation pressure gradient forces), which gives us

$$\frac{\mathrm{d}w}{\mathrm{d}t} = -\frac{1}{\rho}\frac{\partial p}{\partial z} - g. \qquad (1.4)$$

If $\mathrm{d}w/\mathrm{d}t$ is negligible, then (1.4) becomes the so-called *hydrostatic approximation*,

$$\frac{\partial p}{\partial z} = -\rho g. \qquad (1.5)$$

In which types of phenomenon can we assume that $\mathrm{d}w/\mathrm{d}t$ is negligible compared with $|-\frac{1}{\rho}\frac{\partial p}{\partial z}|$ and g? In other words, what determines whether a phenomenon is regarded as a hydrostatic or nonhydrostatic phenomenon?

It turns out we cannot simply scale the individual terms in (1.4) to determine which phenomena are hydrostatic, because the two terms on the rhs are practically always nearly equal in magnitude but opposite in sign, and thus individually are always much larger than their residual (and $\mathrm{d}w/\mathrm{d}t$). To properly assess under which conditions $\mathrm{d}w/\mathrm{d}t$ is negligible, we modify the rhs terms by defining a base state (e.g., an average over a large horizontal area) density and a base state pressure, defined to be in hydrostatic balance with it. We then express the total pressure and density as the sum of the base state value ($\overline{p}$ and $\overline{\rho}$, respectively) and a perturbation (p' and ρ', respectively), that is,

$$p = \overline{p}(z) + p'(x,y,z,t) \qquad (1.6)$$

$$\rho = \overline{\rho}(z) + \rho'(x,y,z,t), \qquad (1.7)$$

and we require

$$0 = -\frac{\partial \overline{p}}{\partial z} - \overline{\rho}g. \qquad (1.8)$$

Multiplying (1.4) by ρ, subtracting (1.8), dividing by ρ, and incorporating the definitions of $\overline{p}$ and $\overline{\rho}$ yields

$$\frac{\mathrm{d}w}{\mathrm{d}t} = -\frac{1}{\rho}\frac{\partial p'}{\partial z} - \frac{\rho' g}{\rho}. \qquad (1.9)$$

The relative importance of $\mathrm{d}w/\mathrm{d}t$ compared with $|-\frac{1}{\rho}\frac{\partial p'}{\partial z}|$ (and $|\frac{\rho' g}{\rho}|$) is

$$\frac{O\left(\frac{\mathrm{d}w}{\mathrm{d}t}\right)}{O\left(-\frac{1}{\rho}\frac{\partial p'}{\partial z}\right)}. \qquad (1.10)$$

The scale of w can be obtained from scaling the continuity equation (the two-dimensional Boussinesq approximation is used for simplicity; see Chapter 2 for a review),

$$O\left(\frac{\partial w}{\partial z}\right) \sim O\left(\frac{\partial u}{\partial x}\right); \tag{1.11}$$

thus,

$$O(w) \sim \frac{VD}{L}, \tag{1.12}$$

where $O(w)$ is the scale of w, and V, D, and L are the characteristic horizontal velocity scale, depth scale, and horizontal length scale of the phenomenon, respectively. From (1.12) the scale of $\mathrm{d}w/\mathrm{d}t$ is therefore

$$O\left(\frac{\mathrm{d}w}{\mathrm{d}t}\right) \sim \frac{VD}{LT}, \tag{1.13}$$

where T is the characteristic timescale for accelerations within the phenomenon.

The scale of $|-\frac{1}{\rho}\frac{\partial p'}{\partial z}|$ may be written as

$$O\left(-\frac{1}{\rho}\frac{\partial p'}{\partial z}\right) \sim \frac{\delta p'}{\rho D}, \tag{1.14}$$

where $\delta p'$ is the characteristic pressure perturbation within the phenomenon. We want to eliminate $\delta p'$ and ρ in favor of the characteristic scales of the phenomenon (e.g., V, D, L, and T). We do this by scaling the horizontal momentum equation as follows:

$$\frac{\mathrm{d}u}{\mathrm{d}t} \approx -\frac{1}{\rho}\frac{\partial p'}{\partial x} \tag{1.15}$$

$$O\left(\frac{\mathrm{d}u}{\mathrm{d}t}\right) \sim O\left(-\frac{1}{\rho}\frac{\partial p'}{\partial x}\right) \tag{1.16}$$

$$\frac{V}{T} \sim \frac{\delta p'}{\rho L} \tag{1.17}$$

$$\frac{VL}{T} \sim \frac{\delta p'}{\rho}; \tag{1.18}$$

therefore, using (1.14),

$$O\left(-\frac{1}{\rho}\frac{\partial p'}{\partial z}\right) \sim \frac{VL}{TD}. \tag{1.19}$$

Using (1.13) and (1.19), (1.10) becomes

$$\frac{O\left(\frac{\mathrm{d}w}{\mathrm{d}t}\right)}{O\left(-\frac{1}{\rho}\frac{\partial p'}{\partial z}\right)} \sim \frac{\frac{VD}{LT}}{\frac{VL}{TD}} = \left(\frac{D}{L}\right)^2. \tag{1.20}$$

The quantity D/L is known as the *aspect ratio* of the phenomenon—the ratio of the characteristic depth scale of the phenomenon to the horizontal length scale (or width) of the phenomenon. When a phenomenon is much wider than it is deep ($D/L \ll 1$), $\mathrm{d}w/\mathrm{d}t$ is relatively small compared with the vertical perturbation pressure gradient force and the phenomenon can be considered a *hydrostatic phenomenon*; that is, the hydrostatic approximation is justified. When a phenomenon is approximately as wide as it is deep ($D/L \sim 1$), $\mathrm{d}w/\mathrm{d}t$ is similar in magnitude to the vertical perturbation pressure gradient force, and the phenomenon is considered a *nonhydrostatic phenomenon*; that is, the hydrostatic approximation should not be made (Figure 1.4). Note that we have assumed equivalent timescales for the horizontal and vertical accelerations [i.e., T is equivalent in (1.13) and (1.17)]. This assumption is equivalent to (1.11), which dictates that D/W (the vertical advective timescale) is equal to L/V (the horizontal advective timescale). There may be cases in which $\partial u/\partial x$ is balanced by $\partial v/\partial y$ such that the scaling in (1.11) is not appropriate. In that case, even phenomena with a large aspect ratio may be nearly hydrostatic. For convective motions, (1.11) is considered a good assumption.

On the synoptic scale, $D/L \sim 10\,\mathrm{km}/1000\,\mathrm{km} \sim 1/100 \ll 1$. On the mesoscale, D/L can be $\sim$1 or $\ll$1, depending on the phenomenon. For example, in a thunderstorm updraft, $D/L \sim 10\,\mathrm{km}/10\,\mathrm{km} \sim 1$ (i.e., the thunderstorm updraft can be considered to be a nonhydrostatic phenomenon). However, for the rain-cooled outflow that the thunderstorm produces, $D/L \sim 1\,\mathrm{km}/10\,\mathrm{km} \sim 1/10 \ll 1$ (i.e., the outflow can be considered to be an approximately hydrostatic phenomenon).

In a hydrostatic atmosphere, pressure can be viewed essentially as being proportional to the weight of the atmosphere above a given point. Pressure changes in a hydrostatic atmosphere arise from changes in the density of air vertically integrated over a column extending from the location in question to $z = \infty$ ($p = 0$). This interpretation of pressure will be useful for some mesoscale phenomena. For a nonhydrostatic phenomenon, we cannot relate pressure fluctuations solely to changes in the weight of the overlying atmosphere. Instead, significant *dynamic* effects may contribute to pressure perturbations. Examples include the low pressure found in the core of a tornado and above the wing of an airplane in flight, and the high pressure found beneath an intense downburst and on the upwind side of an obstacle. The relationship between the pressure field and wind field is discussed in much greater depth in Section 2.5.

In the next chapter we review some of the basic equations and tools that will be relied upon in the rest of the book. The experienced reader may wish to skip ahead to Chapter 3.

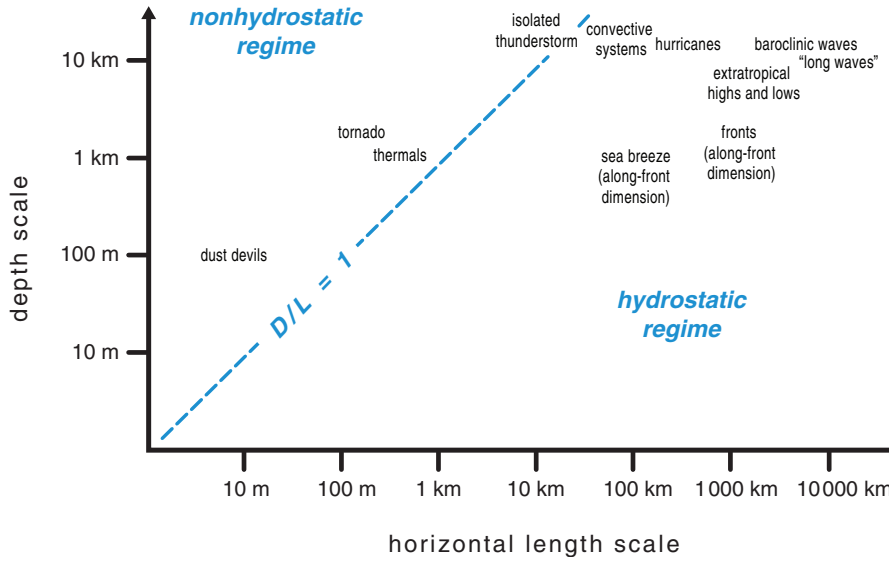

Figure 1.4 We can infer that a phenomenon is hydrostatic when its horizontal length scale is significantly larger than its vertical depth scale. Shown above are some examples of nonhydrostatic and approximately hydrostatic phenomena plotted as a function of depth versus horizontal length (i.e., width) scale.

Further reading

Emanuel (1986).

Fujita, T. T., 1963: Analytical mesometeorology: A review. *Severe Local Storms, Meteor. Monogr.*, No. 27, 77–125.

Fujita (1981).

Fujita, T. T., 1986: Mesoscale classifications: Their history and their application to forecasting. *Mesoscale Meteorology and Forecasting*, P. S., Ray, Ed., Amer. Meteor. Soc., 18–35.

Lilly, D. K., 1983: Stratified turbulence and mesoscale variability of the atmosphere. *J. Atmos. Sci.*, **40**, 749–761.

Maddox (1980).

Orlanski (1975).

Tepper, M., 1959: Mesometeorology—the link between macroscale atmospheric motions and local weather. *Bull. Amer. Meteor. Soc.*, **40**, 56–72.

Thunis, P., and R. Bornstein, 1996: Hierarchy of mesoscale flow assumptions and equations. *J. Atmos. Sci.*, **53**, 380–397.

Vinnichenko, N. K., 1970: Kinetic energy spectrum in the free atmosphere—one second to five years. *Tellus*, **22**, 158–166.